Phenotypic screening of Arabidopsis T-DNA insertion lines for cell wall mechanical properties revealed ANTHOCYANINLESS2, a cell wall-related gene

Phenotypic screening of *Arabidopsis* T-DNA insertion lines for cell wall mechanical properties revealed *ANTHOCYANINLESS2*, a cell wall-related gene

Atsushi Mabuchi, Kouichi Soga, Kazuyuki Wakabayashi and Takayuki Hoson

MABUCHI A, SOGA K, WAKABAYASHI K, & HOSON T. (2016). Phenotypic screening of Arabidopsis T-DNA insertion lines for cell wall mechanical properties revealed ANTHOCYANINLESS2, a cell wall-related gene. *Journal of Plant Physiology*. 191, 29-35. https://doi.org/10.1016/j.jplph.2015.11.011

Phenotypic screening of Arabidopsis T-DNA insertion lines for cell wall mechanical properties revealed *ANTHOCYANINLESS2*, a cell wall-related gene

Atsushi Mabuchi, Kouichi Soga, Kazuyuki Wakabayashi, Takayuki Hoson*

Department of Biology, Graduate School of Science, Osaka City University, Sumiyoshi-ku, Osaka 558-8585, Japan

*Corresponding author. Tel: +81-66605-2577; fax: +81-66605-2577

E-mail address: hoson@sci.osaka-cu.ac.jp (T. Hoson)

ABSTRACT

We performed a phenotypic screening of confirmed homozygous T-DNA insertion lines in Arabidopsis for cell wall extensibility, in an attempt to identify genes involved in the regulation of cell wall mechanical properties. Seedlings of each line were cultivated and the cell wall extensibility of their hypocotyls was measured with a tensile tester. Hypocotyls of lines with known cell wall-related genes showed higher or lower extensibility than those of the wild-type at high frequency, indicating that the protocol used was effective. In the first round of screening of randomly selected T-DNA insertion lines, we identified *ANTHOCYANINLESS2* (*ANL2*), a gene involved in the regulation of cell wall mechanical properties. In the *anl2* mutant, the cell wall extensibility of hypocotyls was significantly lower than that of the wild-type. Levels of cell wall polysaccharides per hypocotyl, particularly cellulose, increased in *anl2*. Microarray analysis showed that in *anl2*, expression levels of the major peroxidase genes also increased. Moreover, the activity of ionically wall-bound peroxidases clearly increased in *anl2*. The activation of peroxidases as well as the accumulation of cell wall polysaccharides may be involved in decreased cell wall extensibility. The approach employed in the present study could contribute to our understanding of the mechanisms underlying the regulation of cell wall mechanical properties.

Keywords: ANTHOCYANINLESS2; Arabidopsis; cell wall extensibility; phenotypic screening; peroxidase; T-DNA insertion line

Introduction

In plants, the cell wall surrounds the cell membrane and provides these cells with structural support and mechanical strength, thereby playing a principal role in diverse plant physiological functions such as growth regulation and environmental responses (Hoson, 2002; Cosgrove, 2005; Wolf et al., 2012). The plant cell wall is composed of various constituents, including cellulose, matrix polysaccharides, phenolics, and structural proteins (Carpita and Gibeaut, 1993). The mechanical properties of the cell wall are determined by the concentrations at which these constituents are present, their molecular size, chemical structure, as well as the complex interactions among them. The synthesis, modification, and degradation of cell wall constituents are mediated by various wall-related enzymes whose activities are regulated by the expression of their genes. Intensive studies have been conducted on cell wall architecture and gene-regulated metabolism of cell wall constituents. Nevertheless, the molecular mechanisms underlying the regulation of the mechanical properties of the cell wall remain to be elucidated.

Genome-wide loss-of-function screening is a powerful approach to clarify unknown gene functions. T-DNA insertion mutants are widely used in Arabidopsis to disrupt gene functioning. The confirmed homozygous T-DNA insertion lines in Arabidopsis, generated by a project at the SALK institute (the Salk Unimutant Collection), are a suitable resource for this purpose (O'Malley and Ecker, 2010). In the present study, we developed the method to explore these T-DNA insertion lines for cell wall mechanical

properties by efficiently cultivating seedlings and measuring cell wall extensibility of their hypocotyls with a tensile tester. A preliminary screening of the T-DNA insertion lines for known cell wall-related genes using the established protocol revealed the utility of this approach. We identified *ANTHOCYANINLESS 2* (*ANL2)*, a gene involved in the regulation of cell wall mechanical properties, by the first round screening of randomly selected T-DNA insertion lines. *ANL2* encodes a homeodomain protein belonging to the HD-GLABRA2 group and may have pleiotropic functions such as an anthocyanin accumulation (Kubo et al., 1999). In rosette leaves of an *anl2* mutant, Nadakuduti et al. (2012) observed a 40% reduction in cutin accumulation. However, a decrease in the cutin level does not explain the decrease in cell wall extensibility of *anl2*. For this reason, we also examined the possible mechanism underlying modifications of cell wall mechanical properties in *anl2*.

Materials and methods

Plant materials and growth conditions

Wild-type *Arabidopsis thaliana* (L.) Heynh. (ecotype Columbia-0) and the confirmed homozygous T-DNA insertion lines of Arabidopsis were used in the present study. T-DNA insertion lines were obtained from the Arabidopsis Biological Resource Center (Columbus, OH, USA). Arabidopsis seeds were planted on 1% (w/v) agar in a 24-well culture plate, and incubated at 4°C for 7 d. The seeds were then exposed to white light

for 1 d at 23°C to induce germination, and cultivated at 24°C in the dark. After cultivation, seedlings were fixed by pouring hot 80% ethanol into each well, and stored in fresh 80% ethanol until further use.

Measurement of hypocotyl length and cell wall extensibility

Before measuring cell wall mechanical properties, seedlings fixed in 80% ethanol were rehydrated with several changes of water and the lengths of their hypocotyls were measured using a scale. The cell wall extensibility of hypocotyls was measured with a tensile tester (Tensilon RTM-25; Toyo Baldwin, Tokyo, Japan) (Parvez et al., 1996). Hypocotyls were fixed between two clamps (distance between clamps was 1 mm) and stretched by lowering the bottom clamp at a speed of 20 mm/min until a load of 0.8 g was produced. Cell wall extensibility (strain/load, μm/g) was determined by measuring the load's rate of increase just before it reached 0.8 g. We selected-T-DNA insertion lines whose cell wall extensibility had increased or decreased by more than 30% from the wild-type, irrespective of significant statistical differences.

Quantification of cell wall polysaccharides

Seedlings (120 per batch) were immediately boiled for 10 min in 80% ethanol after cultivation for quantification of cell wall polysaccharides. Cell wall polysaccharides were fractionated by the methods described by Nishitani and Masuda (1979) and

Sakurai et al. (1987). Hypocotyls excised from rehydrated seedlings were homogenized in water, and then washed with water, acetone and a methanol:chloroform mixture (1:1, v/v), and treated with 2 units/mL porcine pancreatic α-amylase (EC 3.2.1.1; type I-A; Sigma, St. Louis, Mo., USA) in 50 mM sodium acetate buffer (pH 6.5) at 37°C for 3 h. After amylase treatment, pectic substances were extracted from the cell wall material three times (15 min each) with 50 mM EDTA (pH 6.8) at 95°C. Hemicellulose was extracted three times (12 h each) with 4% (w/v) KOH, and three times (12 h each) with 24% (w/v) KOH containing 0.02% $NaBH_4$ at 25°C. The fractions extracted with 4% and 24% KOH were designated as hemicellulose-I and hemicellulose-II, respectively; these fractions were neutralized with acetic acid. The alkali-insoluble fraction (cellulose fraction) was then washed with 0.03 M acetic acid and ethanol, and dried at 40°C. The cellulose fraction was dissolved in 72% (v/v) sulfuric acid for 1 h at 25°C, and then diluted with a 29-fold volume of water. The sugar content in each fraction was determined by the phenol-sulfuric acid method (Dubois et al., 1956) and expressed as glucose equivalents.

Extraction and assay of cell wall-bound peroxidase activity

The collected seedlings (20 per batch) were immediately frozen with liquid nitrogen and kept at -80°C until further use. The frozen seedlings were homogenized with ice-cold 10 mM sodium phosphate buffer (pH 6.8). The homogenate was poured into a plastic column (mini column CC07; Sarstedt, Tokyo, Japan) and then thoroughly

washed with the same buffer. Cell wall residues were then suspended in 10 mM sodium phosphate buffer (pH 6.0) containing 1.5 M NaCl. The suspension was kept for 24 h at 4°C and then filtered through the mini column. The filtrate was used for the assay of the ionically wall-bound peroxidase activity (Wakabayashi et al., 2012). Activity was measured according to the methods outlined in Sato et al. (1993). The reaction mixture (1 mL) contained 50 μL of the enzyme preparation, 13 mM guaiacol, and 5 mM H_2O_2 in 40 mM MES-KOH buffer (pH 6.0). The reaction was initiated by the addition of H_2O_2 at 25°C. The absorbance at 470 nm was recorded at 30 s intervals, and enzyme activity was quantified as the increase in absorbance 1.5 to 2.0 min after the addition of H_2O_2.

Microarray analysis

Seedlings were collected and immediately frozen with liquid nitrogen. Total RNA was extracted using TRIzol Reagent (Invitrogen, Carlsbad, CA, USA) and purified using an RNeasy MinElute Cleanup Kit (Qiagen, Valencia, CA, USA). cDNA and fluorescently labeled cRNA were synthesized using an Affymetrix GeneChip WT PLUS Reagent Kit (Agilent Technologies, Santa Clara, CA, USA). Microarray analysis was performed by Kurabo Industries (Osaka, Japan) with an Arabidopsis Gene 1.0ST Array (Agilent Technologies).

In plants, Class III peroxidases comprise secretory plant peroxidases, and the Arabidopsis genome contains 73 class III peroxidase genes (Tognolli et al., 2002;

Welinder et al., 2002). We analyzed the expression levels of class III peroxidase genes using the values of fluorescence intensities obtained by the microarray analysis.

Phenotype analysis

Wild-type and *anl2* seeds were sown on rockwool blocks moistened with 2000-fold diluted Hyponex solution (Hyponex Japan, Osaka, Japan), and then cultivated under continuous white light (43 ± 2 μmol s^{-1} m^{-2}) at 23°C for 30 d to analyze rosette leaf morphology. Rosette leaves were numbered from the first true leaf that emerged after the cotyledons. Anatomical analysis was carried out using the methods of Kozuka et al. (2011). The leaf blades of the sixth to tenth rosette leaves were detached from the plants. An approximately 2-mm-thick transverse section was sliced at the middle region of the leaf blade by hand-sectioning with a razor blade. Photographs of these sections were taken using a digital multi-angle stereoscopic microscope system (VB-G25; Keyence, Osaka, Japan). An index of leaf flatness was calculated as the ratio of the straight-line distance between the two edges of the leaf blade to the actual width of the leaf blade along the curved surface, as determined using ImageJ software (http://rsbweb.nih.gov/ij/, NIH). Leaf blades of the first to fourth rosette leaves were observed with a scanning electron microscope (TM-1000; Hitachi, Tokyo, Japan) to analyze trichome morphology.

Results

Screening T-DNA insertion lines for cell wall extensibility

A protocol was developed to explore the confirmed homozygous T-DNA insertion lines for cell wall mechanical properties. This consisted of efficient seedling cultivation and sample fixation, and measurement of cell wall extensibility with a tensile tester. The preliminary screening was performed for the T-DNA insertion lines of genes known to encode cell wall proteins, cellulose synthase/cellulose synthase-like protein (*CESA*/*CSL*), xyloglucan endotransglucosylase/hydrolase (*XTH*), laccase (*LAC*), and arabinogalactan protein (*AGP*). Hypocotyls of these lines showed higher or lower cell wall extensibility than the wild-type at high frequency (Fig. S1).

This protocol was then used to screen randomly selected T-DNA insertion lines. We selected lines where cell wall extensibility was increased or decreased by more than 30% from that of the wild-type, irrespective of statistically significant differences (Fig. S2). The lines were also selected for hypocotyl length based on the same standard. In some lines (represented by * in Fig. S2), the change in cell wall extensibility was accompanied by elongation growth. However, other mutants (represented by **) showed changes only in cell wall extensibility.

We performed the first round screening of 405 randomly selected lines, and found that 22 lines showed modifications of cell wall extensibility. We searched the Arabidopsis Information Resource (TAIR) database to determine whether the selected

lines were involved in the regulation of cell wall metabolism. Out of the 22 lines, 11 were classified as “already known” cell wall-related lines, whereas the other 11 were classified as “non-cell wall-related lines” (Table 1). Of the 11 known cell wall-related lines, eight displayed higher cell wall extensibility and three lines had lower extensibility than the wild-type. On the other hand, of the 11 non-cell wall-related lines, seven had higher extensibility and four were lower than the wild-type (Table 1).

Identification of ANL2 as a cell wall-related gene

For the selected lines, cell wall extensibility measurements were repeated at least three times using reproduced seeds to confirm the modifications. As a result, *ANTHOCYANINLESS2* (*ANL2*; AT4G00730, SALK_000196C) was identified as a gene involved in the regulation of cell wall mechanical properties. Cell wall extensibility of hypocotyls for *anl2* was clearly lower than that of the wild-type (Fig. 1). However, no clear differences were detected in the hypocotyl length between the wild-type and *anl2*.

Quantitative changes in cell wall polysaccharides may be one of the possible mechanisms inducing the modification of cell wall extensibility. Cell wall polysaccharides were fractionated into pectin, hemicellulose-I, hemicellulose-II, and cellulose fractions, and their quantities were determined in etiolated hypocotyls of *anl2*. The quantities of all four fractions per hypocotyl or per unit length of hypocotyl significantly increased in *anl2* compared to the wild-type (Fig. 2). In particular, the increase in cellulose level was prominent. Total cell wall polysaccharides in *anl2*

increased by about 60%.

Gene expression levels and activity of peroxidases in anl2

To obtain further a clue to the mechanism underlying the decrease in cell wall extensibility in *anl2*, transcriptional profiles were analyzed by microarray. In *anl2*, the quantity of 13 transcripts was more than twice that of the wild-type (Table S1), whereas that of 49 transcripts was less than 50% of that of the wild-type (Table S2). Because peroxidase genes were included in both categories, we analyzed the expression of class III peroxidase family genes in more detail. In total, 73 sequences encoding class III peroxidase genes have been identified in Arabidopsis (Tognolli et al., 2002; Welinder et al., 2002). Of these, 16 transcripts significantly changed in *anl2*; seven genes were up-regulated, and nine were down-regulated (Fig. 3). The expression level of the major peroxidase gene (i.e., 69) significantly increased in *anl2*. The levels of relatively abundant peroxidase genes, 10, 39, and 59, also increased significantly, whereas those of peroxidase genes 16, 21, and 73 decreased in *anl2*.

We measured the activity of ionically wall-bound peroxidases to determine whether modifications in gene expression reflected its activity because the expression levels of the major, and some other abundant peroxidase genes, were changed in *anl2*. The cell wall-bound peroxidase activity per seedling and per total cell wall polysaccharides significantly increased in *anl2* compared to the wild-type (Fig. 4).

Phenotypic analysis of anl2

Growth phenotypes of *anl2* were analyzed using plants grown under continuous white light conditions. There were no clear differences in the germination rate, plant body height, or the number of lateral branches. However, alterations of trichome morphology and rosette leaves were observed in *anl2* (Fig. 5). The number of trichome branching points was changed in *anl2*, where the number of trichomes with three branching points was increased, and trichomes with two branching points decreased (Fig. 5A, B). No changes were observed in the number of trichomes with one or four branching points (Fig. 5B). On the other hand, rosette leaves were much more curved in *anl2* compared to the wild-type (Fig. 5C). The morphological analysis revealed that leaf flatness was clearly reduced in *anl2* (Fig. 5D).

Discussion

A reliable source of mutant lines and an efficient analytical protocol are required for identifying novel genes involved in the regulation of the cell wall properties in plants. The confirmed homozygous T-DNA insertion lines in Arabidopsis are available as a suitable resource for this purpose (O'Malley and Ecker, 2010). Ryden et al. (2003) developed a sophisticated method to analyze the mechanical properties of Arabidopsis mutants. However, no effective approaches to genome-wide screening for the cell wall

properties previously existed. In the present study, we established an efficient protocol to explore Arabidopsis T-DNA insertion lines relative to their cell wall mechanical properties. We first selected etiolated hypocotyls as a study material because the effects of light are avoidable and they are usable in the short term. The use of a 24-well culture plate also enabled efficient seedling cultivation and sample fixation. Indirect analytical methods, such as curvature or osmotic shock, were first used to examine the mechanical properties of the cell wall. However, these methods were shown to be unreliable when applied to the tiny Arabidopsis seedlings. Thus, we decided to use a conventional tensile tester and a simple stress-strain method for the analysis.

The preliminary screening of T-DNA insertion lines for the known cell wall-related genes, *CESA*/*CSL*, *XTH*, *LAC*, and *AGP*, showed the presence of lines whose cell wall extensibility was modified at high frequency (Fig. S1), indicating the protocol's effectiveness. Our results also suggest that these genes regulate the metabolism of cell wall constituents, thereby contributing to the regulation of cell wall extensibility. Out of these cell wall-related lines, *xth17-1* and *xth17-2* had higher cell wall extensibility in etiolated hypocotyls, whereas the *xth17* line showed reduced petiolar growth rates in response to both low R/FR and green shade (Sasidharan et al., 2010). This discrepancy may be caused by differences in organs and growth conditions. The modification of cell wall extensibility was also observed at a certain rate in the screening of randomly selected T-DNA insertion lines (Fig. S2). In the screening, variations in length among lines were shown to be smaller than those in cell wall extensibility. Growth may be limited by factors other than cell wall mechanical properties, such as osmotic potential,

in lines that show changes only in cell wall extensibility. The cell wall plays a principal role not only in growth regulation, but also in many other physiological processes such as environmental responses. Thus, screening of lines for cell wall extensibility needs to be conducted to understand the mechanism underlying the regulation of cell wall properties.

ANL2 is a gene involved in the regulation of the cell wall mechanical properties that we identified in the first round screening of randomly selected T-DNA insertion lines. The cell wall extensibility of *anl2* hypocotyls was significantly lower than that of the wild-type (Fig. 1). Two *ANTHOCYANINLESS* loci, *ANL1* and *ANL2*, have been reported in Arabidopsis (Kubo et al., 1999, 2007). Both genes are expressed in leaves, stems, flower buds, and roots. *ANL1* encodes UDP-glucose:flavonoid-3-*O*-glucosyltransferase (Kubo et al., 2007), whereas *ANL2* encodes a homeodomain protein belonging to the HD-GLABRA2 group (Kubo et al., 1999). Kubo et al. (1999) suggested that *ANL2* regulates two independent pathways: an anthocyanin accumulation in subepidermal tissues and cellular organization in the primary root. The *ANL2* gene is also involved in cuticle biosynthesis. In rosette leaves of *anl2*, Nadakuduti et al. (2012) observed a 40% reduction in the cutin monomer load and a 25% reduction in the alkane load of cuticle waxes. *GLYCEROL-3-PHOSPHATE ACYLTRANSFERASE 4* (*GPAT4*) and *GPAT6* are involved in cutin biosynthesis in Arabidopsis (Yang et al., 2010). In gene ontology, the term ‘cutin biosynthetic process’ (GO:0010143) has been classified. We analyzed the expression levels of 16 genes with this classification by a microarray analysis (Table S3). Of these genes, *GPAT5 and*

GPAT7 were significantly down-regulated, which may be involved in the inhibition of cutin biosynthesis. In general, a reduced cutin level may lead to softening of the cell wall. Thus, we need to determine other causes contributing to decreases in cell wall extensibility.

Homeodomain proteins also regulate the expression of genes related to the metabolism of cell wall polysaccharides. For example, GLABRA2 (GL2), a member of the HD-GLABRA2 group homeodomain protein family, directly up-regulated the expression of *CESA5* and down-regulated the expression of *XTH17* during root development (Tominaga-Wada et al., 2009). However, the involvement of *ANL2* in the metabolism of cell wall polysaccharides had not yet been reported. In the present study, we showed that the quantity of all four polysaccharide fractions, particularly cellulose, per hypocotyl or per unit length of hypocotyl significantly increased in *anl2*, compared to the wild-type (Fig. 2). The accumulation of cell wall polysaccharides may be involved in a decrease in cell wall extensibility in *anl2*.

Expression levels of major and other abundant peroxidase genes was significantly higher in *anl2* compared to the wild-type (Fig. 3). The ionically wall-bound peroxidase activity per seedling and per total cell wall polysaccharides also increased in *anl2* (Fig. 4). Cell growth is tightly associated with cell wall stiffening and loosing, and the balance between these two processes can be precisely controlled by the antagonistic activities of class III peroxidases (Francoz et al., 2015). Plant class III peroxidases are responsible for oxidizing lignin precursors, including monolignols, lignin oligomers, and polymers (Whetten and Sederoff, 1995; Hoson, 2000; Sasaki et al., 2004;

Fagerstedt et al., 2010). Peroxidases are also involved in cross-linking of the structural hydroxyproline-rich glycoproteins and polysaccharide-bound ferulic acid residues in the cell wall (Fry, 2004; Bunzel, 2010). Changes in the expression of peroxidase genes are known to affect the cell wall architecture. Plants over-expressing *PEROXIDASE 37 (PRX37)* showed an increase in the amount of esterified phenolic material associated with their cell wall (Pedreira et al., 2011). The over-expression of *PRX37* may also decrease cell wall extensibility. In the present study, the signal intensity of *PRX37* increased significantly in *anl2*. In addition, Shigeto et al. (2015) reported that double knockout mutants of *PRX2*, *PRX25*, and *PRX71* had decreased cell wall volume in Arabidopsis stems. On the other hand, hypergravity has been shown to increase cell wall-bound peroxidase activity as well as levels of lignin, thereby decreasing cell wall extensibility (Soga et al., 2001; Wakabayashi et al., 2009; Hoson and Wakabayashi, 2015). Tamaoki et al. (2009) reported that the expression of some peroxidase genes had increased more than two-fold following a hypergravity stimulus. Thus, changes in the expression of class III peroxidases genes, as well as the accumulation of cell wall polysaccharides, may be responsible for the decrease in cell wall extensibility. The native target of increased peroxidases in the cell wall of *anl2* should be determined in future studies.

No clear differences were noted in appearance of light-grown *anl2* plants. However, morphological alterations in trichomes and rosette leaves were observed in *anl2* (Fig. 5). Trichome branching in Arabidopsis is thought to be mediated by transiently stabilized microtubular structures (Mathur and Chua, 2000). In *lefty1* and *lefty2* mutants, which

are caused by dominant-negative amino acid substitutions in α-tubulin, branching of leaf trichomes were highly reduced (Abe et al., 2004). The mutant of katanin, a protein shown to be involved in regulating microtubule disassembly by severing microtubules, was also observed to decrease trichome branching (Burk et al., 2001). Changes in trichome branching in *anl2* may have been caused by alternations of microtubule structures, and *ANL2* may be involved in the regulation of microtubule stability. On the other hand, stiffness of epidermal layers is important for the retention of leaf flatness, and stiffness of epidermal layers is strongly associated with cuticle thickness (Onoda et al., 2015). As mentioned above, the *ANL2* gene is involved in cuticle biosynthesis. Our results suggest that a reduction of cutin accumulation in rosette leaves may cause a decrease in leaf flatness in *anl2*.

In conclusion, we established an efficient protocol to explore T-DNA insertion lines for cell wall mechanical properties in Arabidopsis, and we confirmed *ANL2* as a cell wall-related gene. The possible cause of a decrease in cell wall extensibility in *anl2*, mediated by the accumulation of cell wall polysaccharides and enhanced peroxidase activity, was already known. Novel cell wall-related genes with novel mechanisms may be identified in future studies using the protocol established herein, leading to an understanding of the mechanism underlying the regulation of the cell wall mechanical properties.

Acknowledgements

The present study was supported in part by Grants-in-Aid for Scientific Research (KAKENHI Grant) from the Japan Society for the Promotion of Science.

Appendix A. Supplementary data

Supplementary data associated with this article can be found, in the online version, at http://dx.doi.org/10.1016/j.jplph.2015.11.011.

References

Abe T, Thitamadee S, Hashimoto T. Microtubule defects and cell morphogenesis in the *left1left2* tubulin mutant of *Arabidopsis thaliana*. Plant Cell Physiol 2004;45:211-20.

Burk DH, Liu B, Zhong R, Morrison WH, Ye ZH. A katanin-like protein regulates normal cell wall biosynthesis and cell elongation. Plant Cell 2001;13:5157-62.

Bunzel M. Chemistry and occurrence of hydroxycinnamate oligomers. Phytochem Rev 2010;9:47-64.

Carpita NC, Gibeaut DM. Structural models of primary cell walls in flowering plants: consistency of molecular structure with the physical properties of the walls during growth. Plant J 1993;3:1-30.

Cosgrove DJ. Growth of the plant cell wall. Nat Rev Mol Cell Biol 2005;11:850-61.

Dubois M, Gilles KA, Hamilton JK, Robers PA, Smith F. Colorimetric method for determination of sugars and related substances. Anal Chem 1956;28:350-6.

Fagerstedt KV, Kukkola EM, Koistinen VV, Takahashi J, Marajamma K. Cell wall lignin is polymerized by class III secretable plant peroxidases in Norway spruce. J Integr Plant Biol 2010;52:186-94.

Francoz E, Ranocha P, Nguyen-kim H, Jamet E, Burlat V, Dunand C. Roles of cell wall peroxidases in plant development. Phytochem 2015;112:15-21.

Fry SC. Oxidative coupling of tyrosine and ferulic acid residues: Intra- and extra protoplasmic occurrence, predominance of trimmers and larger products, and possible role in inter-polymeric cross-linking. Phytochem Rev 2004;3:97-111.

Hoson T. Peroxidases. In: Ohnishi M, editor. Glycoenzymes. Tokyo: Japan Scientific

Societies Press, 2000. p 137-47.

Hoson T. Physiological functions of plant cell coverings. J Plant Res 2002;115:277-82.

Hoson T, Wakabayashi K. Role of the plant cell wall in gravity resistance. Phytochem 2015;112:84-90.

Kozuka T, Kong SG, Doi M, Shimazaki K, Nagatani A. Tissue-autonomous promotion of palisade cell development by phototropin 2 in *Arabidopsis*. Plant Cell 2011;23:3684-95.

Kubo H, Peeters AJM, Aarts MGM, Pereira A, Koornneef M. *Anthocyaninless2*. A homeobox gene affecting anthocyanin distributions and root development in Arabidopsis. Plant Cell 1999;11:1217-26.

Kubo H, Nawa N, Lupsea SA. *Anthocyaninless1* gene of *Arabidopsis thaliana* encodes a UDP-glucose:flavonoid-3-*O*-glucosyltransferase. J Plant Res 2007;120:445-9.

Mathur J, Chuna NH. Microtubule stabilization leads to growth reorientation in Arabidopsis trichomes. Plant Cell 2000;12:465-77.

Nadakuduti SS, Pollard M, Kosma DK, Allen C Jr, Ohlrogge JB, Barry CS. Pleiotropic phenotypes of the *sticky peel* mutant provide new insight into the role of *CUTIN DEFICIENT2* in epidermal cell function in Tomato. Plant Physiol 2012;159:945-60.

Nishitani K, Masuda Y. Growth and cell wall changes in azuki bean epicotyls. I. Changes in wall polysaccharides during intact growth. Plant Cell Physiol 1979;20:63-74.

O'Malley RC, Ecker JR. Linking genotype to phenotype using the Arabidopsis unimutant collection. Plant J 2010;61:928-40.

Onoda Y, Schieving F, Anten NP. A novel method of measuring leaf epidermis and mesophyll stiffness shows the ubiquitous nature of the sandwich structure of leaf laminas in broad-leaved angiosperm species. J Exp Bot 2015;66:2487-99.

Parvez MM, Wakabayashi K, Hoson T, Kamisaka S. Changes in cellular osmotic potential and mechanical properties of cell walls during light-induced inhibition of cell elongation in maize coleoptiles. Physiol Plant 1996;96:179-85.

Pedreira J, Herrera MT, Zarra I, Revilla G. The overexpression of *AtPrx37*, an apoplastic peroxidase, reduces growth in *Arabidopsis*. Physiol Plant 2011;141:177-87.

Ryden P, Sugimoto-Shirasu K, Smith AC, Findlay K, Reiter W-D, McCann MC. Tensile properties of Arabidopsis cell walls depend on both a xyloglucan cross-linked microfibrillar network and rhamnogalacturonan II-borate complexes. Plant Physiol 2003;132:1033-40.

Sakurai N, Tanaka S, Kuraishi S. Changes in wall polysaccharides of squash (*Cucurbita maxima* Duch.) hypocotyls under water stress condition. I. Wall sugar composition and growth as affected by water stress. Plant Cell Physiol 1987;28:1051-8.

Sasaki S, Nishida T, Tsutsumi Y, Kondo R. Lignin dehydrogenative polymerization mechanism: A poplar cell wall peroxidase directly oxidizes polymer lignin and produces in vitro dehydrogenative polymer rich in beta-*O*-4 linkage. FEBS Lett 2004;562:197-201.

Sasidharan R, Chinnappa CC, Staal M, Elzenga JTM, Yokoyama R, Nishitani K, Voesenek LACJ, Pierik R. Light quality-mediated petiole elongation in Arabidopsis during shade avoidance involves cell wall modification by xyloglucan endotransglucosylase/hydrolases. Plant Physiol 2010;154:978-90.

Sato Y, Sugiyama M, Gorecki RJ, Fukuda H, Komamine A. Interrelationship between lignin deposition and the activities of peroxidase isoenzymes in differentiating tracheary elements of *Zinnia*. Planta 1993;189:584-9.

Shigeto J, Itoh Y, Hirao S, Ohira K, Fujita K, Tsutsumi Y. Simultaneously disrupting *AtPrx2, AtPrx25 and AtPrx71* alters lignin content and structure in *Arabidopsis* stem. J Integr Plant Biol 2015;57:349-56.

Soga K, Wakabayashi K, Hoson T, Kamisaka S. Gravitational force regulates elongation growth of Arabidopsis hypocotyls by modifying xyloglucan metabolism. Adv Space Res 2001;27:1011–6.

Tamaoki D, Karahara I, Nishiuchi T, De Oliveira S, Schreiber L, Wakasugi T, Yamada K, Yamaguchi K, Kamisaka S. Transcriptome profiling in *Arabidopsis* inflorescence stems grown under hypergravity in term of cell walls and plant hormones. Adv Space Res 2009;44:245-53.

Tognolli M, Penel C, Greppin H, Simon P. Analysis and expression of the class III peroxidase large gene family in *Arabidopsis thaliana*. Gene 2002;288:129-38.

Tominaga-Wada R, Iwata M, Sugiyama J, Kotake T, Ishida T, Yokoyama R, Nishitani K, Okada K, Wada T. The GLABRA2 homeodomain protein directly regulates *CESA5* and *XTH17* gene expression in Arabidopsis roots. Plant J 2009;60:564-74.

Wakabayashi K, Nakano S, Soga K, Hoson T. Cell wall-bound peroxidase activity and lignin formation in azuki bean epicotyls grown under hypergravity conditions. J Plant Physiol 2009;166:947-54.

Wakabayashi K, Soga K, Hoson T. Phenylalanine ammonia-lyase and cell wall peroxidase are cooperatively involved in the extensive formation of ferulate network in

cell walls of developing rice shoots. J Plant Physiol 2012;169:262-7.

Welinder KG, Justesen AF, Kjærsgård IVH, Jensen RB, Rasmussen SK, Jerpersen HM, Duroux L. Structural diversity and transcription of class III peroxidases from *Arabidopsis thaliana*. Eur J Biochem 2002;269:6063-81.

Whetten R, Sederoff R. Lignin biosynthesis. Plant Cell 1995;7:1001-13.

Wolf S, Hématy K, Höfte H. Growth control and cell wall signaling in plants. Annu Rev Plant Biol 2012;63:381-407.

Yang W, Pollard M, Li-beisson Y, Beisson F, Feig M, Ohlrogge J. A distinct type of glycerol-3-phosphate acyltransferase with sn-2 preference and phosphatase activity producing 2-monoacylglycerol. Proc Natl Acad Sci USA 2010;107:12040-5.

Figure legends

Fig. 1. Cell wall extensibility (A) and length (B) of hypocotyls of an *anl2* mutant. Seedlings grown for 36 h in the dark were harvested and the length and cell wall extensibility of hypocotyls was measured. Data are means ± SE (n = 23). * Mean value was significantly different between the wild-type (WT) and *anl2* mutants at the 5% level (Student's t-test).

Fig. 2. Amounts of cell wall polysaccharides in *anl2*. Seedlings were grown as described in Fig. 1, and cell wall polysaccharides were fractionated into four fractions. Sugar contents in each fraction per hypocotyl (A) and per unit length of hypocotyl (B) were determined by the phenol-sulfuric acid method using glucose as the standard. Data are means ± SE (n = 4). * Mean value was significantly different between the wild-type (WT) and *anl2* at the 5% level (Student's t-test).

Fig. 3. Expression levels of class III peroxidase genes. Seedlings were grown as described in Fig. 1, and the expression levels of class III peroxidase genes were analyzed using fluorescence intensity values obtained through a microarray analysis described in the Materials and Methods. Peroxidase genes whose intensity values are significantly different between the wild-type and *anl2* plants are presented (i.e., *PRX10*, AT1G49570; *PRX16*, AT2G18980; *PRX17*, AT2G22420; *PRX20*, AT2G35380; *PRX21*, AT2G37130; *PRX22*, AT2G38380; *PRX28*, AT3G03670; *PRX37*, AT4G08770; *PRX38*,

AT4G08780; *PRX39*, AT4G11290; *PRX52*, AT5G05340; *PRX56*, AT5G15180; *PRX59*, AT5G19890; *PRX69*, AT5G64100; *PRX73*, AT5G67400). Data are means ± SE (n = 4).

Fig. 4. Activity of cell wall-bound peroxidases (PRX) in *anl2*. Seedlings were grown as described in Fig. 1. Activities per seedling (A) and per total cell wall polysaccharides (B) were measured using guaiacol as the substrate and expressed as the increase in the absorbance at 470 nm. Data are means ± SE (n = 5). * Mean values were significantly different between the wild-type (WT) and *anl2* at the 5% level (Student's t-test). CW, cell wall.

Fig. 5. Morphology of rosette leaves of *anl2*. Rosette leaves obtained from 30-d-grown plants were used for the analysis. Trichome morphology (A) was observed using a scanning electron microscope; scale bar = 100 μm. Proportion of trichome branching points (B). The percentage of branching points was calculated for approximately 800 trichomes from five rosette leaves. Curling of a rosette leaf, where the transverse section of the rosette leaf blade was observed using a stereoscopic microscope; scale bar = 1 mm (C). Rosette leaf flatness was analyzed according to the methods described in the Materials and methods (D). Data are means ± SE (n = 25). * Mean values were significantly different between the wild-type (WT) and *anl2* at the 5% level (Student's *t*-test).

Table 1. T-DNA insertion lines selected in the present study.

Locus	Stock number	Gene description	Cell wall extensibility (% of WT)
Cell wall-related genes			
Higher cell wall extensibility			
AT1G65310	SALK_008429C	Xyloglucan endotrans-glucosylase/hydrolase 17	140
AT2G32540	SALK_067582C	Cellulose synthase-like protein B4	128
AT2G41905	SALK_148775C	Protein match is Arabino-galactan protein 23	127
AT3G20865	SALK_089247C	Arabinogalactan protein 40	129
AT4G24000	SALK_008597C	Cellulose synthase-like protein G2	150
AT5G10430	SALK_024865C	Arabinogalactan protein 8	146
AT5G40730	SALK_046558C	Arabinogalactan protein 24	121
AT5G48100	SALK_002972C	Laccase-like 15	131
Lower cell wall extensibility			
AT1G32180	SALK_037261C	Cellulose synthase-like protein D6	66
AT2G32530	SALK_025333C	Cellulose synthase-like protein B3	76
AT4G00730	SALK_000196C	Anthocyaninless 2	57
Non-cell wall-related genes			
Higher cell wall extensibility			
AT1G32950	SALK_013864C	Subtilase family protein	148
AT1G55020	SALK_000058C	Lipoxygenase	120

AT1G66860	SALK_014047C	Class I glutamine amido-transferase-like superfamily protein	131
AT1G67960	SALK_000924C	Pollen defective in guidence 1	127
AT3G02810	SALK_000019C	Receptor-like cyto-plasmic kinase	167
AT4G17780	SALK_000834C	F-box and associated interaction domains-containing protein	150
AT5G03070	SALK_005888C	Putative importin alpha isoform	147
Lower cell wall extensibility			
AT3G10090	SALK_006148C	Nucleic acid-binding, OB-fold-like protein	73
AT3G30570	SALK_000350C	Non-LTR retrotrans-poson family	68
AT4G02280	SALK_016906C	Sucrose synthase 3	63
AT4G08050	SALK_000344C	Gypsy-like retrotrans-poson family	73

Fig. 1

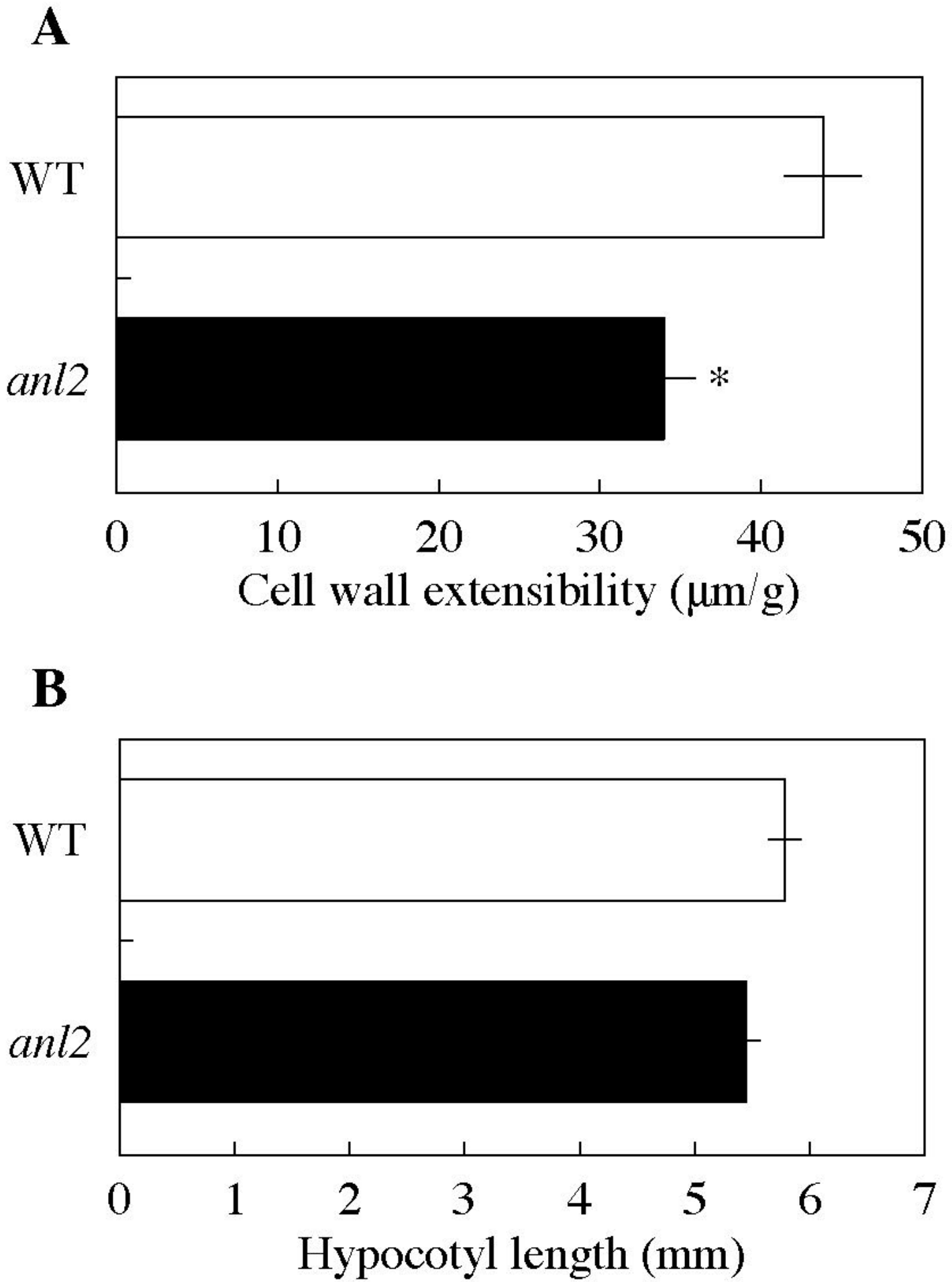
A
WT
anl2
*
0
10
20
30
40
50
Cell wall extensibility (μm/g)
B
WT
anl2
0
1
2
3
4
5
6
7
Hypocotyl length (mm)

Fig. 2

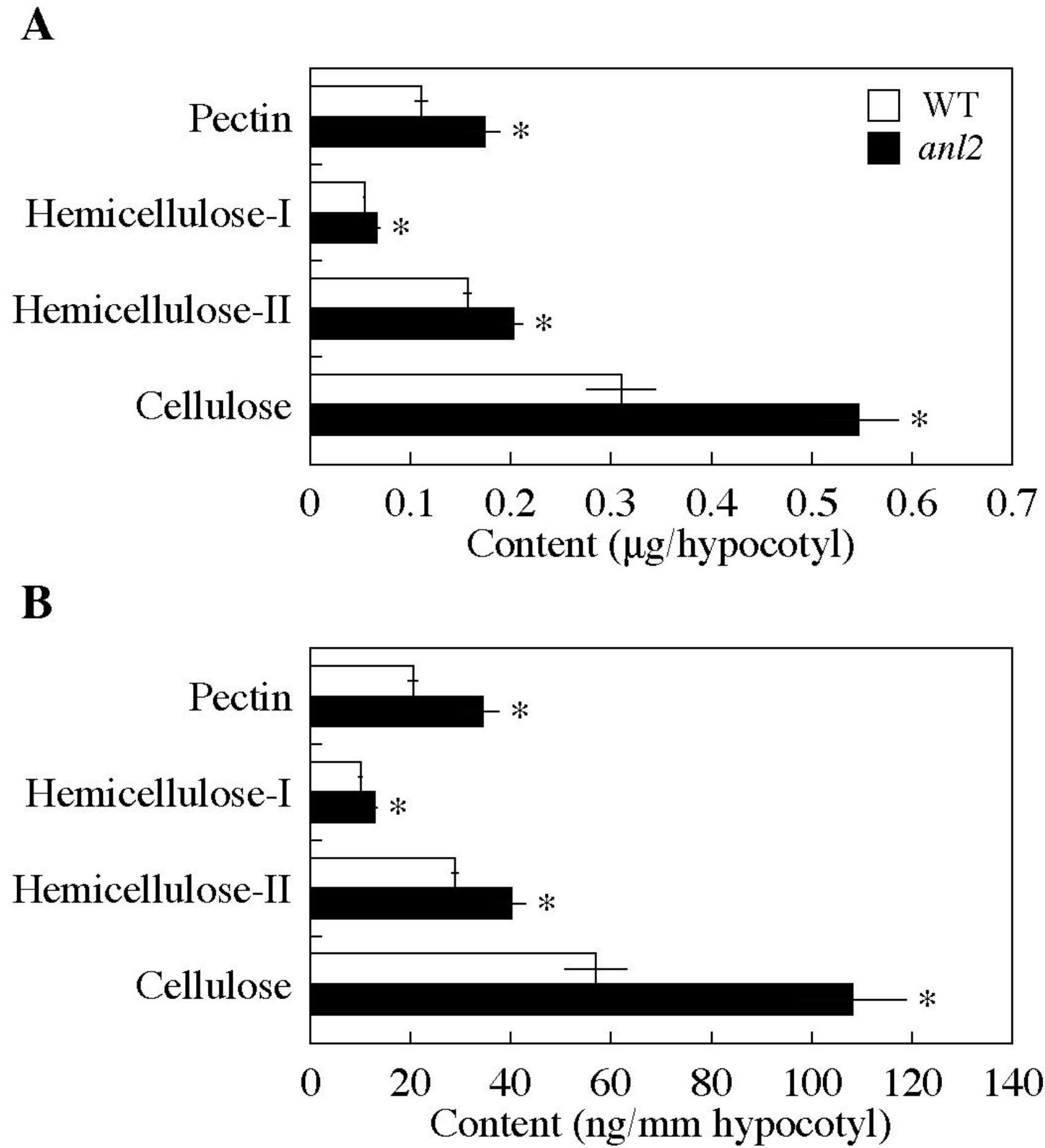
A
Pectin
Hemicellulose-I
Hemicellulose-II
Cellulose
WT
anl2
*
0
0.1
0.2
0.3
0.4
0.5
0.6
0.7
Content (μg/hypocotyl)
B
Pectin
Hemicellulose-I
Hemicellulose-II
Cellulose
*
0
20
40
60
80
100
120
140
Content (ng/mm hypocotyl)

Fig. 3

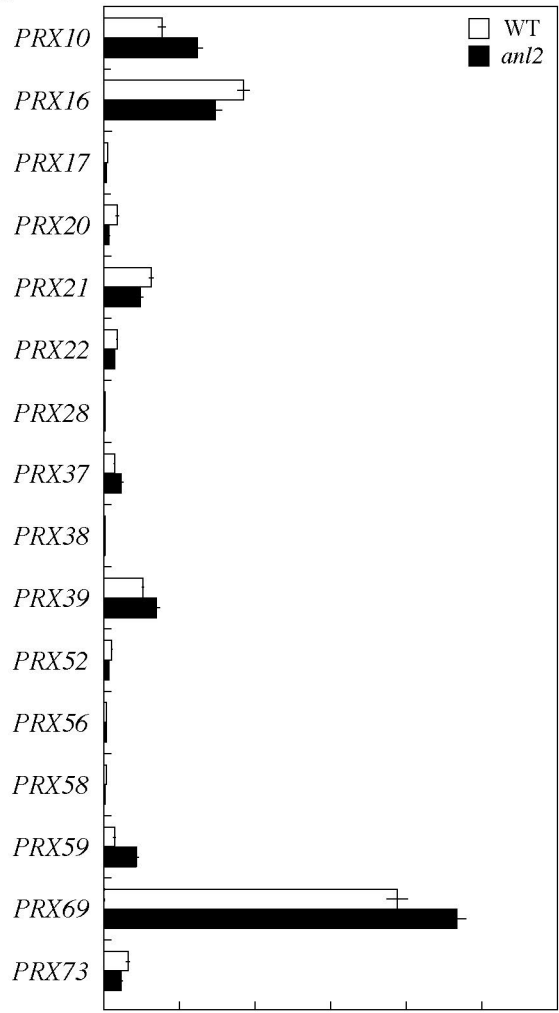
WT
anl2
PRX10
PRX16
PRX17
PRX20
PRX21
PRX22
PRX28
PRX37
PRX38
PRX39
PRX52
PRX56
PRX58
PRX59
PRX69
PRX73
0
100
200
300
400
500
600
Signal intensity

Fig. 4

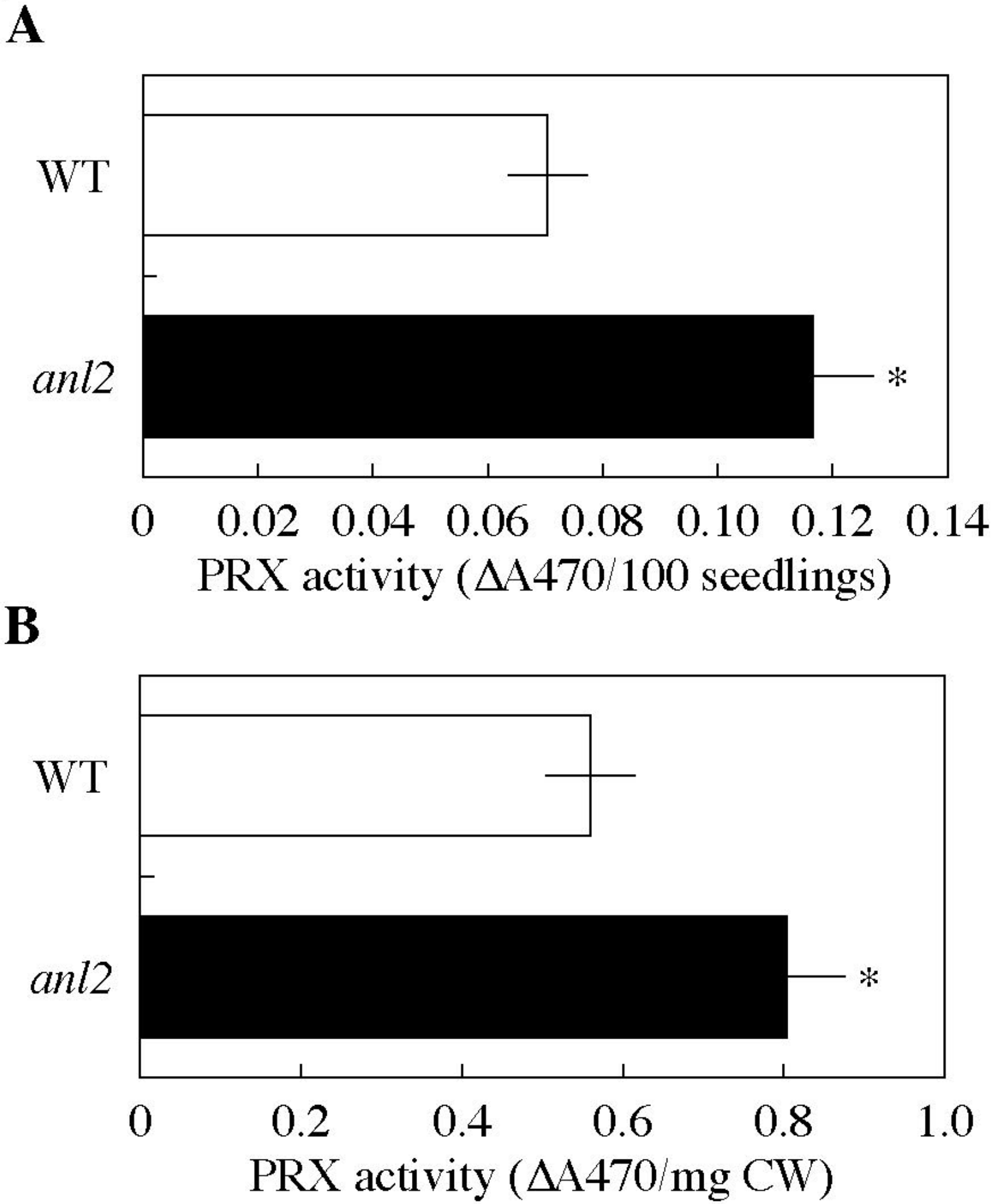
A
WT
anl2
*
0
0.02
0.04
0.06
0.08
0.10
0.12
0.14
PRX activity (ΔA470/100 seedlings)
B
WT
anl2
*
0
0.2
0.4
0.6
0.8
1.0
PRX activity (ΔA470/mg CW)

Fig. 5

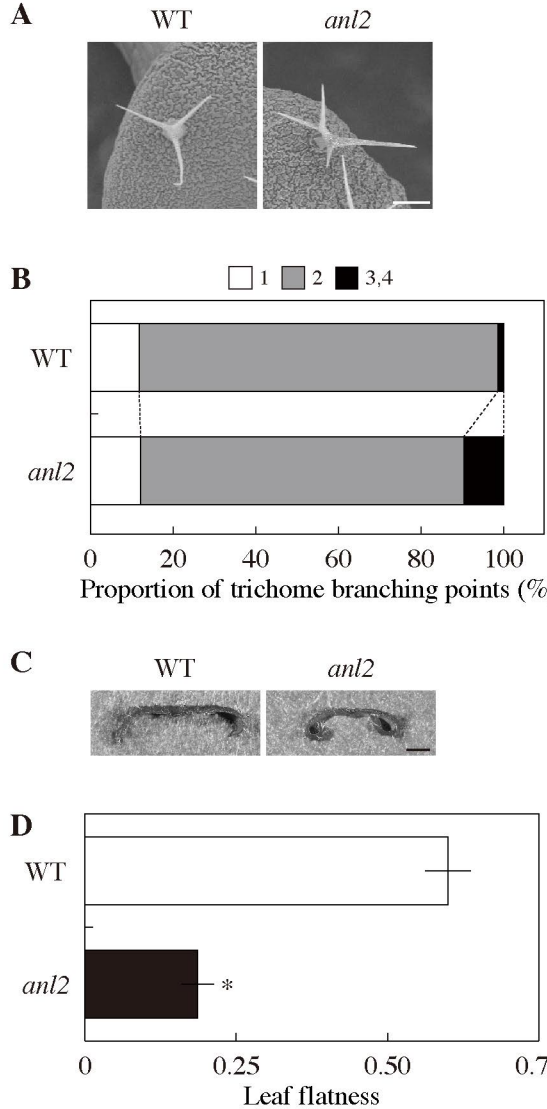
A
WT
anl2
B
1
2
3,4
WT
anl2
0
20
40
60
80
100
Proportion of trichome branching points (%)
C
WT
anl2
D
WT
anl2
*
0
0.25
0.50
0.75
Leaf flatness